Numerical Analysis of Parametric Variations in an Asymmetrically Heated Contra Rotating Disc System

Afaque Ahmed Bhutto[*], Iftikhar Ahmed Bhutto[†], Abdul Fatah Abbasi[‡], Israr Ahmed[§], Samiullah Qureshi[**], Mujeeb-U-Ddin Memon Sahrai[††]

Abstract

To minimize the cost of jet engines, future generations of ultra-high bypass engines may utilize counter-rotating disc systems. This research investigated the fluid stream and heat transfer behaviour between an asymmetrically heated counter-rotating plate system. For the analysis of the parameters, simulation work has been according to the experimental work found in the literature. Results are obtained for Reynolds number and mass stream rates with a plate velocity ratio of -1. The commercial software ANSYS Fluent is implemented employing the axisymmetric, constant state and elliptical method of the cylindrical polar coordinate system. The low-Re number "$k-\varepsilon$" and the low-Re number 2nd moment closure model, are invoked to analyze the fluid stream and heat transfer behaviour between counter-rotating discs. The simulation results illustrate the stream structure, static temperature profiles, and Nusselt number as Reynolds numbers and mass streams change. The stream structure predicted by the two turbulence models shows fluid cores circulating between laminar boundary layers. These centres formed a two-cell structure that cancelled each other in the central part of the cavity. The current stream parameter is a key parameter that affects the stream structure, static temperature and Nusselt number. The Nusselt numbers predicted by the two turbulence models are in good condition with experimental measurements.

Keywords: Contra Rotating Disc System; Low Reynolds Number; Second Moment Closure; Heat Transfer; Numerical Simulations

Introduction

Gas turbine engines play a crucial role in various industrial applications, from electricity generation to aircraft power. The efficiency and effectiveness of these engines are strongly influenced by the complex interplay of heat transfer and fluid dynamics within these components,

[*]Department of Basic Science and Related Studies, The University of Larkano, Larkana 77150, Pakistan, afaq_bhutto@uolrk.edu.pk

[†]Department of Mathematics, Sukkur IBA University, Kandhkot Campus, Kandhkot 79165, Pakistan. iftikhar.kdk@iba-suk.edu.pk

[‡]Department of Mechanical Engineering, Mehran University of Engineering and Technology Jamshoro, Jamshoro 76062, Pakistan, afatah66@yahoo.com

[§]Department of Mathematics, Shah Abdul Latif University, Khairpur 66111, Pakistan, israr.memon@salu.edu.pk

[**]Department of Mechanical Engineering, Mehran University of Engineering and Technology Jamshoro, Jamshoro 76062, Pakistan. samiullah@faculty.muet.edu.pk

[††]Sindh Madressatul Islam University, Karachi 74000, Pakistan, mujib63@hotmail.com

especially for rotating disc systems (Abbasi, Memon, & Pathan, 2012). Understanding and optimizing these phenomena is critical to improving thermal efficiency, extending engine life, and reducing maintenance costs (Szybist et al., 2021). Recent advances in turbine technology, such as increased turbine inlet temperatures and pressure ratios, have greatly improved the operating parameters of gas turbine engines (Sirignano & Liu, 1999). However, these improvements also resulted in higher temperatures experienced by critical components such as turbine blades, nozzle guide covers and rotor-stator plates, which caused thermal stress to develop. As a result, solving the thermal management challenges caused by these high temperatures has become an important focus for gas turbine designers (Mai & Ryu, 2021). Many Researchers and engineers has worked on the numerical and experimental work related to the heat transfer and fluid flow (Bhutto et al., 2023; Ruiz et al. 2021; Bhutto et al., 2022; Rafiq et al., 2020; Bilal et al., 2022; Shamshuddin et al., 2019; Bhutto et al., 2024; Khokhar et al., 2023; Kumar et al., 2022; Bendjaghlouli et al., 2019). Optimizing the thermal efficiency and creating an efficient internal air-cooling system, different researchers performed their experiments and studied numerically to this field. In recent years, researchers have increasingly turned to experimental and numerical studies to investigate heat transfer and fluid stream in rotating plates. These studies aim to elucidate the underlying physics of fluid motion, temperature distribution, and heat transfer mechanisms in these complex systems. Using advanced CFD techniques and experimental methods, researchers can simulate and analyse complex stream patterns and thermal behaviour in rotating plate systems.

In the asymmetrical heated rotating disc, the rotationally induced resilience force is very influential because this force transports the fluid from heated disc to the freezing one via the central core region notorious as axial wind (Memon et al., 1999; Poncet & Serre, 2009). The basic stream structure and entry of hot conventional gas into the rotor-stator disc space was described by Owen and Rogers (1995). Rotor-stator systems have several important characteristics, Gan et al., (1993) pointed out the access problem associated with the system. The development of computer resources and simulation techniques facilitated the development of more detailed and realistic models of rotating disc systems. High-fidelity simulations allow researchers to capture complex stream phenomena, including boundary layer separation, secondary streams, and turbulence effects. Such comprehensive simulations provide valuable insights into the complex interactions between fluid motion and heat transfer, paving the way for improved design strategies and advanced thermal management techniques". Chen et al. (1997) conducted a comprehensive examination

of fluid flow dynamics and heat transfer within a contra-rotating disc system across various Re numbers and mass flow rates. Our investigation delves into simulating the fluid dynamics and heat transfer phenomena within a similar contra-rotating disc setup, with a dual-disc configuration serving as our focal point. We have employed two distinct turbulence models within the fluent, low Re number 2nd moment closure model and the $low\ \ Re$ number "$k-\varepsilon$" model. This approach enables a clear understanding of the complex fluid behaviour and thermal characteristics within the system.

Problem Description and Boundary Conditions

The experimental study provides geometric parameters that closely adhere to the specifications These parameters are: "$s = 0.046m$", "$b = 0.381\,m$", "$ri = 0.05\,m$", "$sc = 0.004\,m$", & "$G = 0.12$" where "s, b, ri", & "sc" represent the axial separation, outer radius, of the discs, respectively. Plates, inner radius, axial difference between the two plates and gap ratio. In the experimental study (Chen et al., 1997), the thermal gradient of the slabs shows an asymmetry that gradually increases with the radial expansion of the slab. Specifically, the left (heated) plate withstands 100 °C, while the right (cooled) plate remains at 20 °C. Similarly, the inlet coolant temperature is assumed to correspond to the cold plate temperature of 20 °C.

Numerical Method

To calculate the discretized transport equation, a row-by-row approach based on the three-diagonal matrix algorithm (TDMA) is used in the assessment procedure. Until the axial and radial moment equations are resolved on the tripping mesh, all variables are resolved at the nodes of the main mesh. A SIMPLEC algorithm (Doormaal & Raithby, 1984) is used to simplify the pressure field and rectify velocity values to ensure mass continuity. Numerous researchers (Abbasi et al., 2012; Javiya et al., 2012; Memon et al., 1999; Morse, 1989, Morse, 1991; Roy et al., 2001; Doormaal & Raithby, 1984; Wang et al., 2023) have made significant strides in discretizing the transport equations through the implementation of a control volume approach alongside a higher-order linear upwind separation scheme (Castro & Jones, 1987). This approach involves modifying the near-wall regions, such as discs and shrouds, to establish a wall distance which is non-dimensional ($i.e. y^+ = yU\tau/\nu$, where "y", "$U\tau$" and "ν" characterize the simplified wall distance, rapidity velocity, and kinematic viscosity, separately). The condition $y^+ < 0.5$ confirms a proper division of nodes in the neighbouring-wall regions, thereby optimizing the computational accuracy. Opting for non-uniform grids is a

more reliable and cost-effective approach. The use of a non-uniform fine grid comprising 75×92 points in the axial and radial tendencies is essential for all prognostications, according to Figure 1.The identical grid layout employed by (Abbasi et al., 2012; Gan et al., 1993) for isothermal modelling of rotating disc systems.

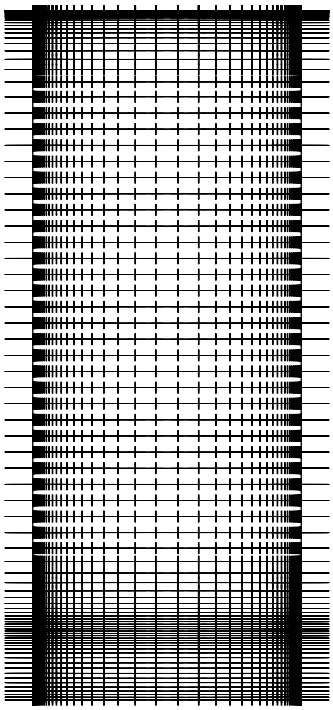

Figure 1: Non-uniform grid arrangement.

Governing Equations

The governing equation of the momentum and energy of axisymmetric and regular stream in a cylindrical polar coordinate system are expressed in terms of the general variable "Φ" as:

$$\frac{\partial}{\partial z}(\rho\, U\, \Phi) + \frac{1}{r}\frac{\partial}{\partial r}(r\, \rho\, V\, \Phi) = \frac{\partial}{\partial z}\left(\Gamma_{\Phi,\mathrm{r}}\,, \frac{\partial \Phi}{\partial z}\right) + \frac{1}{r}\frac{\partial}{\partial r}\left(r\, \Gamma_{\Phi,\mathrm{r}}\,, \frac{\partial \Phi}{\partial r}\right) + \boldsymbol{S}_c \tag{1}$$

with the continuity equation:

$$\frac{\partial}{\partial z}(\rho\, U) + \frac{1}{r}\frac{\partial}{\partial r}(r\, \rho\, V\,) = 0 \tag{2}$$

Low Reynolds number "$k - \varepsilon$" model, and energy equation for describing the second moment were employed to calculate the calculations; these models are automatically integrated into the Ansys fluent. The following details describe the turbulence modelling and its equation with energy.

Low Reynolds Number k-ε Model

The model "$k-\varepsilon$",which is a two-equation low Reynolds number and derived from the transport equations governing both the kinetic energy "k" and its decay "ε" ,was developed from those references (Jones & Launder, 1973, 1972; Launder & Sharma, 1974):

$$\rho\overline{U_\iota U_J} = \frac{2}{3}\,\delta_{ij}\,\rho\,k - \mu_\intercal\left[\frac{\partial U_i}{\partial x_j} + \frac{\partial U_j}{\partial x_i} - \frac{2}{3}\,\delta_{ij}\nabla.\underline{V}\right] \quad (3)$$

where "$\nabla.\underline{V}$ is the divergence of the velocity vector",

$$\nabla.\underline{V} = \frac{\partial U}{\partial z} + \frac{\partial V}{\partial r} + \frac{V}{r} \quad (4)$$

where normal stresses are expressed as "$\frac{2}{3}\,\delta_{ij}$".

Second Moment Closure with a Low Reynolds Number

The model for closed-circuit scenarios with low Re numbers, expressed in (Lai & So, 1990), does not account for the deficiency of isotropic eddy viscosity. This modelling framework employ Reynolds stress closure, which is a method that solves for transport equations in the near-wall region using Cartesian tensor notation as:

$$\frac{\partial}{\partial x_j}\left(\rho U_i U_j\right) = -\frac{\partial p}{\partial x_i} + \frac{\partial}{\partial x_j}\left(\mu\frac{\partial U_i}{\partial x_j} - \rho\overline{U_\iota U_J}\right) \quad (5)$$

where, U_i is the component of mean, and "U_j" is the component of variable velocity, "P" suggest static pressure, "ρ" is the liquid density and "μ" is the viscosity. Since the turbulence model, "$\overline{U_\iota U_J}$" denotes the six components of the Re stress tensor.

$$\frac{\partial}{\partial x}\,(\rho\,U\,\varphi) + \frac{1}{r}\,\frac{\partial}{\partial r}(r\,\rho\,V\,\varphi) = \frac{\partial}{\partial x}\left(\mu\frac{\partial\varphi}{\partial x}\right) + \frac{1}{r}\,\frac{\partial}{\partial r}\left(r\,\mu\,\frac{\partial\varphi}{\partial r}\right) + s_\varphi \quad (6)$$

Energy Equation

A general representation of the Reynolds-averaged energy equation for constant turbulent stream can be provided by means of Cartesian tensor notation as:

$$\frac{\partial}{\partial x_j}\left(U_j\,\varphi\right) = \frac{\partial}{\partial x_j}\left(\frac{\mu}{p_r}\,\frac{\partial\varphi}{\partial x_j} - \overline{U}_J\,\varphi\right) \quad (7)$$

The governing equation for transportation beyond, extending from the principles of momentum and energy conservation for a steady and axisymmetric flow, can be elegantly transformed into a cylindrical polar coordinate system. This transformation allows for a universal representation in terms of the variable φ:

$$\frac{\partial}{\partial x}\,(U\,\varphi) = \frac{1}{r}\frac{\partial}{\partial r}(r\,V\,\varphi) = \frac{\partial}{\partial x}\left(\frac{\mu}{p_r}\,\frac{\partial\varphi}{\partial x}\right) + \frac{1}{r}\frac{\partial}{\partial r}\left(\frac{r\mu}{p_r}\,V\,\frac{\partial\varphi}{\partial r}\right) + s_\varphi \quad (8)$$

where the source term "s_φ" and turbulent heat flux tensor is occurred in Equation (8).

Discussion of Numerical Results

The simulated results of both models explain the computed stream formations of the fluid stream, the computed static temperature contours, computed local Nusselt numbers and the computed moment coefficients.

Computed stream structure

Figure 2 (a-c) illustrates the calculated stream formations of two models across 3 different values of rotating Reynolds numbers ($R_{e\theta} = 2.09 \times 10^5, 2.10 \times 10^5$ and 2.24×10^5) along with mass stream rates "$C_w = 3939612$ and 9718", sustaining a constant rate of disc speed ratio "$\Gamma = -1$". Upon analysing these stream formations, it appears that the recirculating cores of fluid are located between the boundary layers and the mid-plane shear region. Therefore, a configuration featuring two-cell stream formations has been delineated within this specific region. A stagnation point is formed when these cells of counter rotation are removed by streamlines and lines cancelling each other at the outer region of the cavity. Outcomes of that laminar boundary layers have been produced on both the discs and turbulent in stream in the central of disc space. These stream structures exhibited the stability with the Re analogy of the contra-rotating disc stream system as indicated by Chen et al., (1997). These stream models are heavily concerned by mass stream and Re number commonly identified as turbulent stream parameters, $\lambda_T (\lambda_T = C_w R_{e\theta}^{-0.8})$. For higher turbulent stream parameter $\lambda_T = 0.510$, a convincing wall-jet is modelled on the warm disc, which transport the warm from blistering disc to cooling fluid than to freezing disc. It is attributed that for higher mass stream and Re number more heat can be transfer from heated disc to freezing fluid.

Identify the Headings

In Figure 3(a-c), the static temperature contours of two models are shown for three different values of rotating Re numbers ("$R_{e\theta} = 2.09 \times 10^5, 2.10 \times 10^5$" & "$2.24 \times 10^5$") mass stream rate "$C_w = 3939612$" and 9718. As indicated by Figure 3a, the source region of the cavity with a low turbulent stream parameter ""$\lambda_T = 0.218$"" recirculates a lesser amount of fluid at the initial stage. As a result, the lowest temperature circulation occurs here in comparison to the exterior region of the cavity. Therefore, less heat is transmitted from the heated to freezing disc at earlier stage of the cavity.

At higher rotational Re number "$R_{e\theta} = 2.10 \times 10^5$", and mass stream rate, "$C_w = 6121,55\%$" rise in the turbulent stream parameter "$\lambda_T = 0.338$". For these higher stream conditions, a robust wall-jet is modelled happening heated disc accordingly, most important chunk of the

fluid stimulated along the intense disc in radial path and outstanding part moved along the freezing disc. The temperature division from the heated disc to fluid is also improved as demonstrated in the Figure 3b. The heat is transferred from hot disc to cold fluid.

Figure 3c depicts the computed static temperature contours for "$\lambda_T = 0.510$" turbulent stream parameter, which is "135%" excessive than the first case "$\lambda_T = 0.218$". For this high stream parameter, a strong source region and wall-jet is formed in the cavity result of that robust recirculation cell of the fluid is moulded along the heated disc which dominated the right-side cell of the fluid. Due to this, the temperature partition in this region is also raised, resulting in a greater transfer of heat. The contrast between double models illustrates that the Re stress model expected higher warm transfer in the external chunk of the cavity than the "$k - \varepsilon$" model.

Calculated Nusselt number

Figure 4(a-c) describes the difference between the calculated and evaluated Nusselt numbers for three values of turbulent stream parameters, "$\lambda_T = 0.218$", "$\lambda_T = 0.338$" and "$\lambda_T = 0.510$" respectively. Figure.4a depicts the comparison of calculated and measured Nusselt numbers for the turbulent stream parameter "$\lambda_T = 0.218$" for lower rotating Reynolds number, "$R_{e\theta} = 2.09 \times 10^5$" and mass stream rate "$C_w = 3939$" .The Reynolds pressure version anticipated the highest Nusselt quantity value on a hollow space inlet under drift conditions". This Nusselt quantity value denoted that the incoming axial fluid go with the drift at once impacted the new disc, engendering a sturdy wall jet alongside stated disc and facilitating warmth switch from the new disc to the fluid. Initially, the heated fluid underwent opposite move withinside the supply area and mingled with the bloodless fluid, precipitating a speedy decline in computed Nusselt numbers withinside the opposite path inside this area. In contrast, the "$k - \varepsilon$" version did not mirror the height Nusselt quantity stage on this area. Comparative evaluation of the 2 fashions shows that the Reynolds pressure version aligns properly with the findings of (Chen et al., 1997), mainly withinside the outer hollow space area, while the "$k - \varepsilon$" version underperforms. Figure. 4b explains difference of predicted and measured Nusselt numbers for turbulent stream parameter $\lambda_T = 0.338$. At extreme rotational Re numbers, such as $R_{e\theta} = 2.09 \times 10^5$ and above, coupled with higher mass stream rates where $C_w = 6121$, both theoretical frameworks anticipate that the Reynolds stress model will yield higher Nusselt numbers during the initial stages within the cavity. Elevated Nusselt numbers signify that with increased mass stream, the intensity of the liquid-wall jet amplifies, consequently impacting the extent of the

source region, which expands throughout the recirculation area. A comparative analysis between the two models reveals that the Reynolds stress model aligns well with experimental measurements, whereas the "$k-\varepsilon$" model tends to underestimate the entire stream region except for the outer cavity area.

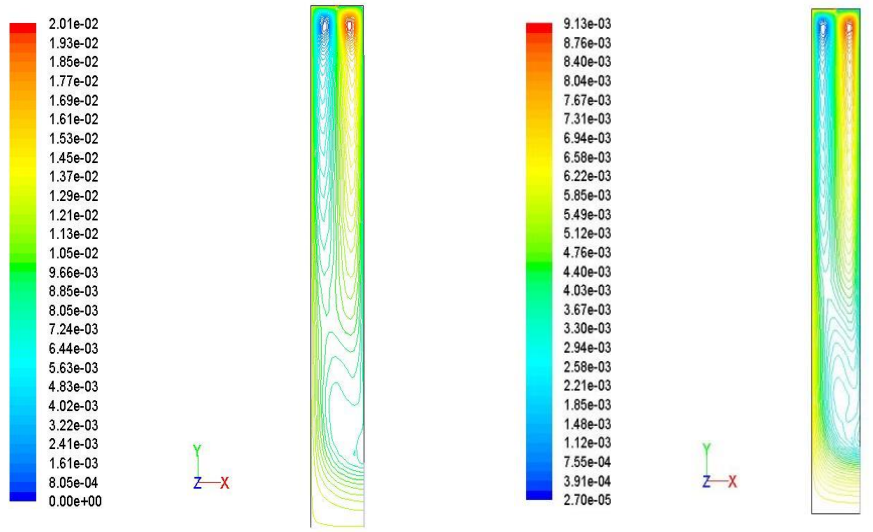

(a)

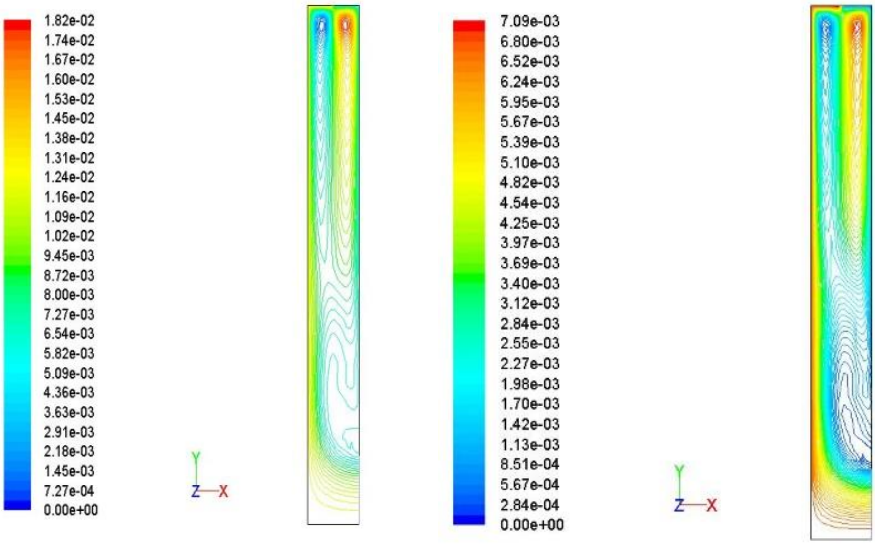

(b)

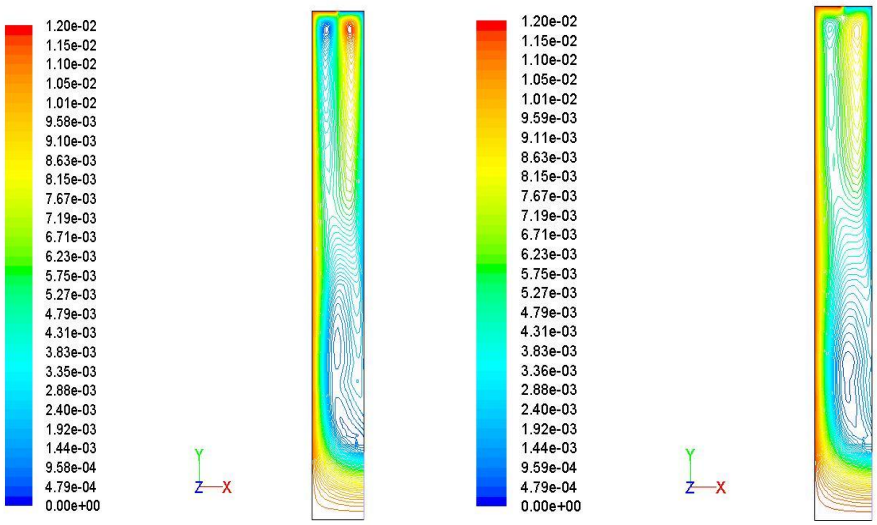

(c)

Figure 2: Analysis of the computed stream formations for (a) "$Re\theta = 2.09 \times 105$" "$Cw = 3939$" (b) "$Re\theta = 2.10 \times 105$," "$Cw = 6121$" and (c) "$Re\theta = 2.24 \times 105$" "$Cw = 9718$" for disc haste ratio, "$\Gamma = -1$"

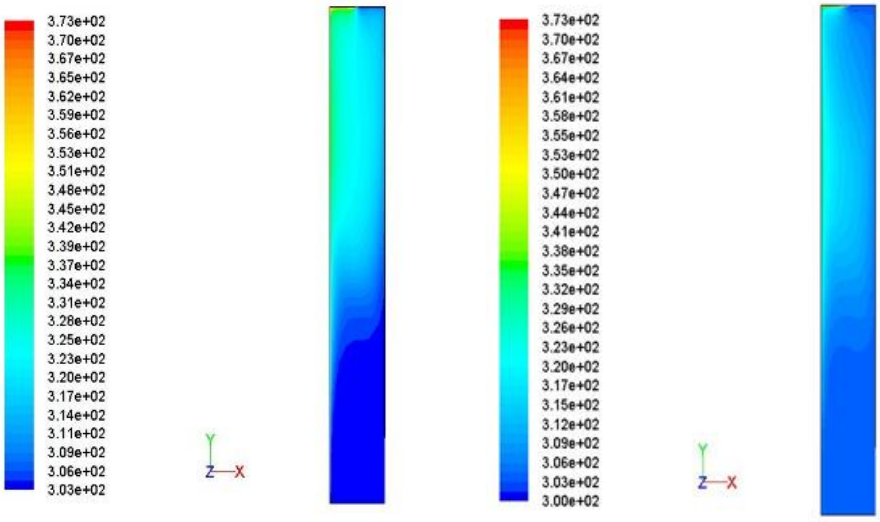

(a)

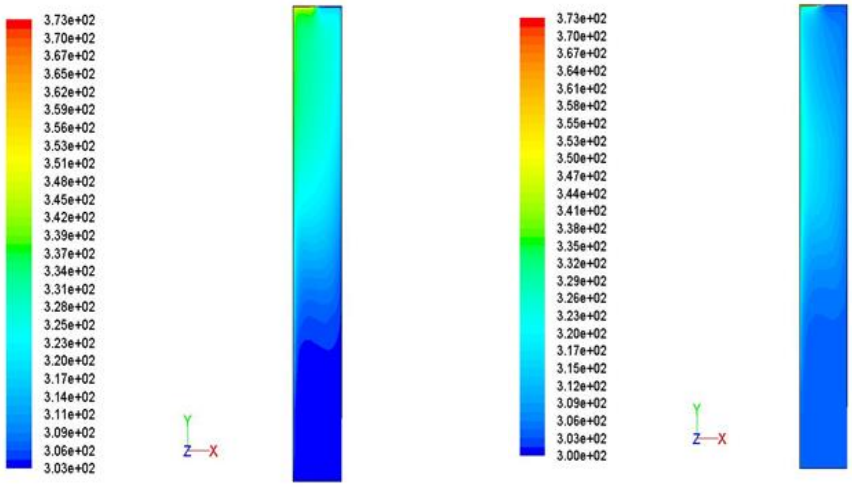

(b)

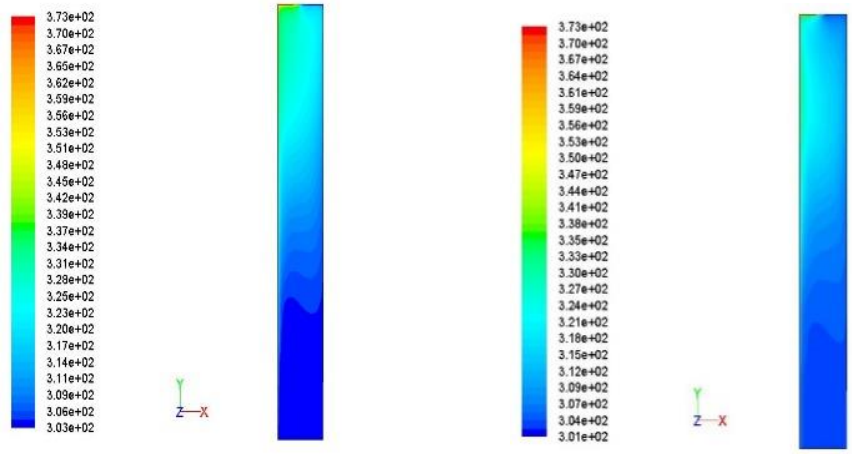

(c)

Figure 3: Analysis of the calculated invariable temperature contours
(a) $R_{e\theta} = 2.09 \times 10^5$, ***"***$C_w = 3939$***"***
(b) "$R_{e\theta} = 2.10 \times 10^5$***", "***$C_w = 6121$***" and***
(c) "$R_{e\theta} = 2.24 \times 10^5$***", "***$C_w = 9718$***", for disc haste ratio, "***$\Gamma = -1$***".***

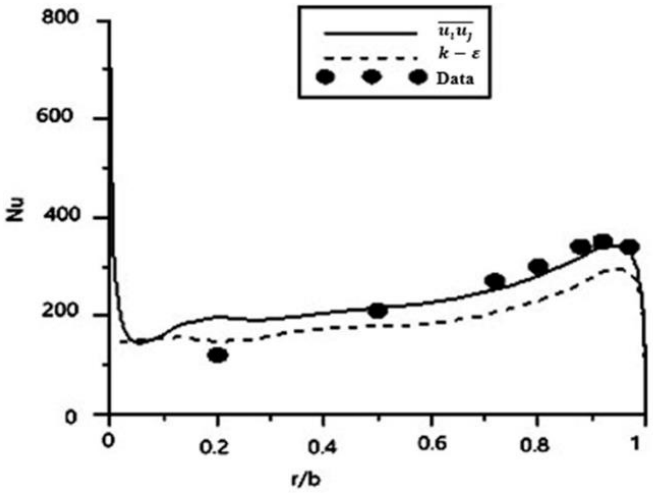
800
600
400
200
0
Nu
0
0.2
0.4
0.6
0.8
1
r/b
$\overline{u_i u_j}$
$k-\varepsilon$
Data

(a)

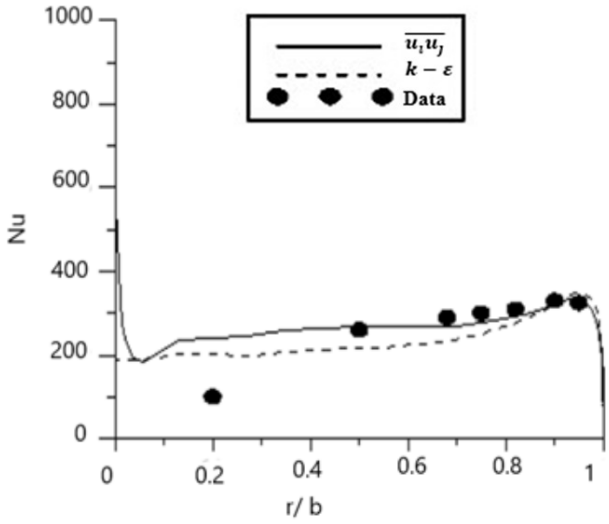
1000
800
600
400
200
0
Nu
0
0.2
0.4
0.6
0.8
1
r/ b
$\overline{u_i u_j}$
$k-\varepsilon$
Data

(b)

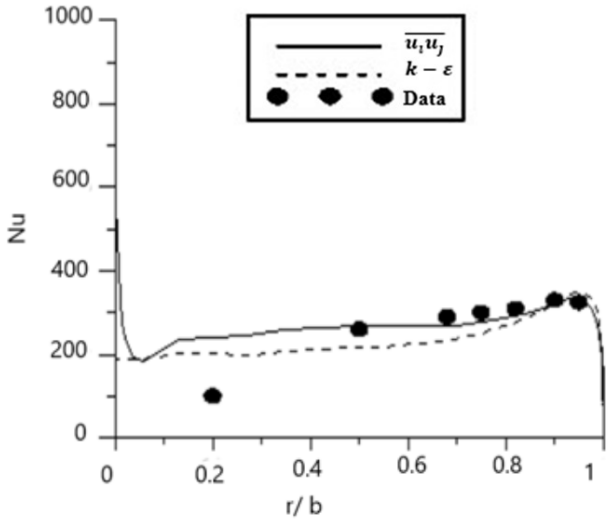

(c)

Figure 4: Comparison of calculated and determined Nusselt numbers for three parameters of turbulent streams.

In the realm of turbulent flows, characterized by a stream parameter $\lambda_T = 0.510$, exhibits a notable increase of 134% compared to the initial scenario. This augmentation correlates with a corresponding elevation in computed Nusselt numbers, mirroring trends elucidated in prior analyses. Notably, both computational models exhibit a propensity for higher Nusselt numbers under these intensified flow conditions. However, a comparative analysis with empirical data unveils a tendency towards overestimation by both models during the initial phase of cavity formation, attributable to the heightened turbulence therein. Consequently, the Reynolds stress model demonstrates superior alignment with experimental measurements (Chen et al., 1997), particularly within the middle and outer extents of the cavity.

Conclusion

Several non-isothermal counter-rotating plate streams were examined for their rotational Reynolds numbers and mass stream parameters. The study investigated the effect of these parameters on the calculated stream configuration, temperature profiles and Nusselt numbers. The analysis revealed the presence of four separate stream regions, paying special attention to the source region, which showed

sensitivity to the turbulent stream parameter $\lambda_{\mathrm{T}}\left(\lambda_{\mathrm{T}} = C_w R_{e\theta}^{-0.8}\right)$ showing a continuous increase. In particular, the elevated turbulent stream parameters induced a strong wall jet along the heated plate, which facilitated significant heat transfer. As a result, the maximum temperature distribution was concentrated on the heating plate. The Reynolds stress model showed the highest Nusselt number values at the radial origin, indicating the direct axial stream effect on the hot plate and the subsequent heat transfer through the solid wall jet. In the initial phase, the Nusselt number rapidly decreased in the opposite direction, which meant that the hot liquid circulated in the source region and mixed with the colder liquid. Comparative analysis of the models showed favourable agreement with measurements from previous studies. Significant differences appeared in the source region, highlighting the superiority of the low-Reynolds second-moment closure model in predicting complex stream patterns and achieving converged solutions. Hence, it is apparent that the second-moment closure model is particularly effective for complex and wall-bounded shear streams, especially at low Reynolds numbers.

References:

Abbasi, A. F., Memon, M., & Baloch, A. (2012). Modelling and Predictions of Isothermal Flow Inside the Closed Rotor-Stator System. *Mehran University Research Journal of Engineering & Technology*, *31*(1).

Abbasi, A. F., Memon, M., & Pathan, D. M. (2012). Numerical Prediction of Closed Contra-Rotating Disc Flows. *Mehran University Research Journal of Engineering & Technology*, *31*(4).

Bhutto, A. A., Ahmed, I., Rajput, S. A., & Shah, S. A. R. (2023). *The effect of oscillating streams on heat transfer in viscous magnetohydrodynamic MHD fluid flow*. *VFAST Transactions on Mathematics.*

Ruiz, D., Mueller, D., & Abu-Mulaweh, H. (2021, November). Modeling and Simulation of Convective Heat Transfer Caused by a Rotating Disk. In ASME International Mechanical Engineering Congress and Exposition (Vol. 85673, p. V011T11A079). American Society of Mechanical Engineers.

Bhutto, A. A., Harijan, K., Hussain, M., Shah, S. F., & Kumar, L. (2022). Numerical Simulation of Transient Combustion and the Acoustic Environment of Obstacle Vortex-Driven Flow. *Energies 2022, Vol. 15, Page 6079*, *15*(16), 6079. https://doi.org/10.3390/EN15166079

Rafiq, T., Mustafa, M., & Farooq, M. A. (2020). Modeling heat transfer in fluid flow near a decelerating rotating disk with variable fluid

properties. International Communications in Heat and Mass Transfer, 116, 104673.

Bilal, M., Marwat, D. N. K., & Alam, A. (2022). Diffusion of heat and mass in flow of viscous fluid over a moving porous and rotating disk. Advances in Mechanical Engineering, 14(8), 16878132221119917.

Shamshuddin, M. D., Mishra, S. R., Bég, O. A., & Kadir, A. (2019). Numerical study of heat transfer and viscous flow in a dual rotating extendable disk system with a non-Fourier heat flux model. Heat Transfer—Asian Research, 48(1), 435-459.

Bhutto, I. A., Bhutto, A. A., Khokhar, R. B., Soomro, M. A., & Shaikh, F. (2023). *The effect of uniform and exponential streams on Magnetohydrodynamic flows of viscous fluids. VFAST Transactions on Mathematics.*

Bhutto, I. A., Khan, I., Furqan, M., Alzahrani, A. H., Bhutto, A. A., & Singh, A. (2024). Wall film cooling mechanism in liquid fuel combustion chamber containing gaseous hydrogen. *International Journal of Hydrogen Energy*, *52*, 246–255.

Castro, I. P., & Jones, J. M. (1987). Studies in numerical computations of recirculating flows. *International Journal for Numerical Methods in Fluids*, *7*(8), 793–823.

Chen, J.-X., Gan, X., & Owen, J. M. (1997). *Heat transfer from air-cooled contrarotating disks*.

Gan, X., Kilic, M., & Owen, J. M. (1993). Flow and heat transfer between gas-turbine discs. *AGARD CONFERENCE PROCEEDINGS AGARD CP*, 25.

Javiya, U., Chew, J. W., Hills, N. J., Zhou, L., Wilson, M., & Lock, G. D. (2012). *CFD analysis of flow and heat transfer in a direct transfer preswirl system*.

Jones, W. P., & Launder, B. (1973). The calculation of low-Reynolds-number phenomena with a two-equation model of turbulence. *International Journal of Heat and Mass Transfer*, *16*(6), 1119–1130.

Jones, W. P., & Launder, B. E. (1972). The prediction of laminarization with a two-equation model of turbulence. *International Journal of Heat and Mass Transfer*, *15*(2), 301–314.

Kumar, M., & Mondal, P. K. (2022). Irreversibility analysis of hybrid nanofluid flow over a rotating disk: Effect of thermal radiation and magnetic field. Colloids and Surfaces A: Physicochemical and Engineering Aspects, 635, 128077.

Bendjaghlouli, A., Ameziani, D. E., Mahfoud, B., & Bouragbi, L. (2019). Magnetohydrodynamic counter rotating flow and heat transfer in

a truncated conical container. Journal of Thermophysics and Heat Transfer, 33(3), 865-874.

Khokhar, R. B., Bhutto, A. A., Siddiqui, N. F., Shaikh, F., & Bhutto, I. A. (2023). *Numerical analysis of flow rates, porous media, and Reynolds numbers affecting the combining and separating of Newtonian fluid flows*.

Lai, Y. G., & So, R. M. C. (1990). On near-wall turbulent flow modelling. *Journal of Fluid Mechanics*, *221*, 641–673.

Launder, B. E., & Sharma, B. I. (1974). Application of the energy-dissipation model of turbulence to the calculation of flow near a spinning disc. *Letters in Heat and Mass Transfer*, *1*(2), 131–137.

Mai, T. D., & Ryu, J. (2021). Effects of damaged rotor blades on the aerodynamic behavior and heat-transfer characteristics of high-pressure gas turbines. *Mathematics*, *9*(6), 627.

Memon, M. D., Memon, A. A., & Jokhio, M. H. (1999). Application of the low Reynolds number second moment closure to the closed rotor-stator flows. *MEHRAN UNIVERSITY RESEARCH JOURNAL OF ENGINEERING AND TECHNOLOGY*, *18*, 117–126.

Morse, A. P. (1989). Application of a low Reynolds number k-ϵ turbulence model to high-speed rotating cavity flows. *Turbo Expo: Power for Land, Sea, and Air*, *79139*, V001T01A073.

Morse, A. P. (1991). *Assessment of laminar-turbulent transition in closed disk geometries*.

Owen, J. M., & Rogers, R. H. (1995). Flow and heat transfer in rotating disc systems, Vol. 2: Rotating Cavities. *Mechanical Engineering Research Studies, Engineering Design Series*.

Poncet, S., & Serre, É. (2009). High-order LES of turbulent heat transfer in a rotor–stator cavity. *International Journal of Heat and Fluid Flow*, *30*(4), 590–601.

Roy, R. P., Xu, G., & Feng, J. (2001). A study of convective heat transfer in a model rotor–stator disk cavity. *J. Turbomach.*, *123*(3), 621–632.

Sirignano, W. A., & Liu, F. (1999). Performance increases for gas-turbine engines through combustion inside the turbine. *Journal of Propulsion and Power*, *15*(1), 111–118.

Szybist, J. P., Busch, S., McCormick, R. L., Pihl, J. A., Splitter, D. A., Ratcliff, M. A., Kolodziej, C. P., Storey, J. M. E., Moses-DeBusk, M., & Vuilleumier, D. (2021). What fuel properties enable higher thermal efficiency in spark-ignited engines? *Progress in Energy and Combustion Science*, *82*, 100876.

Van Doormaal, J. P., & Raithby, G. D. (1984). Enhancements of the

SIMPLE method for predicting incompressible fluid flows. *Numerical Heat Transfer, 7*(2), 147–163.

Wang, R., Gao, F., Chew, J. W., Marxen, O., & Sun, Z. (2023). Advanced modelling of flow and heat transfer in rotating disc cavities using open-source CFD. *Turbo Expo: Power for Land, Sea, and Air*, *87011*, V07BT14A009.